Journal of Natural Gas Science and Engineering 18 (2014) 451–466

Contents lists available at ScienceDirect

Journal of Natural Gas Science and Engineering

journal homepage: www.elsevier.com/locate/jngse

Impact of matrix swelling area propagation on the evolution of coal permeability under coupled multiple processes

Hongyan Qu[a,b], Jishan Liu[c,*], Zhejun Pan[d], Luke Connell[d]

[a] State Key Laboratory of Petroleum Resources and Prospecting, China University of Petroleum, 18 Fuxue Road, Changping, Beijing 102249, China
[b] State Key Laboratory of Geomechanics and Geotechnical Engineering, Institute of Rock and Soil Mechanics, Chinese Academy of Sciences, Wuhan 430071, China
[c] School of Mechanical and Chemical Engineering, The University of Western Australia, 35 Stirling Highway, Perth, WA 6009, Australia
[d] CSIRO Earth Science and Resource Engineering, Private Bag 10, Clayton South, Victoria 3169, Australia

ARTICLE INFO

Article history:
Received 19 October 2013
Received in revised form
10 April 2014
Accepted 12 April 2014
Available online 7 May 2014

Keywords:
Coal permeability
Temperature
Gas sorption
Swelling area
Coupled multiphysics

ABSTRACT

In coal permeability models, it is normally assumed that coal matrix pressure is equalized with the fracture pressure (local equilibrium). In this assumption, coal swells uniformly under constant confining (total) stress conditions commonly used in laboratory measurements. Under these conditions, a uniform swelling will not change the fracture aperture for a matchstick model where only two sets of vertical fractures cut through the whole matrix blocks. However, a uniform swelling changes both the fracture aperture and the spacing (the coal bridge swelling increases the fracture aperture while the matrix swelling changes the spacing only) for a fractured coal model, where fractures do not create a full separation between adjacent matrix blocks but where solid coal bridges are present, is used. Therefore, coal permeability remains unchanged for a matchstick model or increases slightly due to the coal bridge swelling under common laboratory conditions. These conclusions are directly contradictory with most laboratory observations in the literature. This direct contradiction suggests that the local equilibrium condition has not been achieved under common laboratory conditions. If this was the case, the current local equilibrium assumption based approach would be inappropriate for the analysis of laboratory measurements.

In our previous studies, we introduced a concept of matrix swelling transition from local to global under stress conditions. In this concept, we recognized the fact that coal permeability evolves as a function of time from the initial equilibrium state (both matrix pressure and fracture pressure are equal to the initial reservoir pressure) to the final equilibrium state (both matrix pressure and fracture pressure are equal to the injection pressure). In this study, we extended this concept to the most complex situations where multiple processes (thermal transport, gas transport and coal deformation) are involved. Based on the concept of matrix swelling transition, we introduced a new concept of Critical Swelling Area that defines the relationship between swelling transition and coal permeability evolution. The combination of swelling transition and Critical Swelling Area concepts can explain why adsorptive types of gas injection reduces coal permeability in the early stage of the injection and may rebound later.

1. Introduction

Coal permeability models are essential to characterize the coal seam gas production and CO_2 sequestration in coal seams (Pan and Connell, 2012). In these models, the most widely applied assumptions are uniaxial strain and constant stress (Gray, 1987).

The uniaxial strain boundary condition is where strain within the horizontal plane is zero but vertical strain may occur (Palmer and Reeves, 2007). The uniaxial strain conditions were assumed in many prevalent models (Clarkson et al., 2008, 2010; Cui and Bustin, 2005; Gray, 1987; Palmer and Mansoori, 1996; Pan and Connell, 2011; Palmer et al., 2007; Pekot and Reeves, 2002; Seidle and Huitt, 1995; Shi and Durucan, 2004a,b) and were considered suitable for the in-situ coal seam conditions.

The constant volume condition is another widely used boundary condition, where the increase in the volume of the coal matrix due to coal swelling would be equal to the decrease in that of the fracture aperture (Ma et al., 2011). Under the constant volume assumption, 100% of coal swelling due to the CO_2 injection should contribute to the decrease of coal permeability. The concept of

* Corresponding author. Tel.: +61 430 136 986.
E-mail address: jishan.liu@uwa.edu.au (J. Liu).

http://dx.doi.org/10.1016/j.jngse.2014.04.007
1875-5100/

constant volume reservoirs was applied by Harpalani and Chen (1995), who developed a simplified permeability model by using this theory (Ma et al., 2011). Massarotto et al. (2009) also suggested that the coalbed reservoirs may be under a constant volume condition.

Together with the uniaxial strain, the constant stress has been widely employed in boundary conditions, where the stress due to the weight of the overburden geology overlying a reservoir does not change. Models that can be applied to the stress controlled boundary conditions were developed recently (Connell and Detournay, 2009; Connell et al., 2010; Liu and Rutqvist, 2010; Liu et al., 2010a, 2011a; Izadi et al., 2011; Ma et al., 2011; Massarotto et al., 2009; Robertson and Christiansen, 2006). Under the constant stress condition, the external boundary is allowed to expand. Therefore, only part of the coal swelling would contribute to changes in coal permeability.

Laboratory efforts were made to observe permeability evolutions in coal since measurements are easier to obtain and often considered alternatives to field measurements for model validation. Mitra et al. (2012) is the first and probably the only one so far to report experimental study under uniaxial strain condition. Their experiment replicated in situ conditions where the bulk sample was not permitted to shrink as a result of gas desorption by adjusting the confining pressure. The results showed that coal permeability increases continuously with the decrease of gas pressure. The experimental data was used to validate the widely used Shi & Durucan and Palmer permeability models (Liu et al., 2012). However, neither of the models matches the experimental data well.

Most other previous experiments were conducted under the constant stress conditions, where the samples were allowed to deform axially as well as radially (Vishal et al., 2013a,b; Kiyama et al., 2011; Viete and Ranjith, 2006; Wang et al., 2010; Mazumder and Wolf, 2008). Measurements by Moffat and Weale (1955) showed that the swelling strain increases with gas pressure and then decreases after reaching a maximum, while the adsorption approaches a plateau at high pressures. This behavior is a combined effect of adsorption-induced swelling and compression of coal solid by gas pressure (Pan and Connell, 2007). Laboratory observations (Pini et al., 2009; Robertson, 2005; Siriwardane et al., 2009) have shown that coal permeability under the influence of gas adsorption can change instantaneously from reduction to enhancement at the constant stress conditions.

It is commonly believed that this instantaneous switching of permeability is due to the fact that the matrix swelling ultimately ceases at higher pressures and the influence of effective stress takes over given that the fracture permeability is mainly affected by both effective stress and sorption-induced swelling. Under the constant stress boundary condition, the decrease in the effective stress due to the increase in the pore pressure tends to open the fractures and enhances permeability. Meanwhile, the coal matrix swelling caused by the large adsorption capacity narrows the fractures, leading to a reduction in permeability. The net change of permeability is a result of the competition between these two combined effects. However, the effect of the effective stress can be easily overestimated (Liu et al., 2010a; Qu et al., 2012).

Three permeability models, Shi & Durucan model, Palmer & Mansoori model, and Seidle & Huitt model, were used to fit the permeability results in Robertson's experiment (Robertson, 2005). However the model fits were not good, because the experimental conditions were different from the assumed uniaxial strain condition of these models. Izadi et al. (2011) proposed a model, the results from which also demonstrated that under stress controlled conditions the injection of adsorptive gases reduces the coal permeability at a lower gas pressure while the coal permeability might rebound at a higher gas pressure. They attributed the permeability reduction to the predominant sorption-induced strain at low pressure and permeability rebound to the decrease of the effective stress due to the increase of pore pressure. However, even though the results may match the experiment observations to some extent, the reason may not be precise.

Liu and Harpalani (2013a,b) presented a theoretical approach to model sorption-induced coal shrinkage and swelling and incorporated it into the permeability prediction models. The model first calculates the theoretical coal matrix shrinkage strain. Using the calculated strain, various commonly used permeability models are applied to two sets of field data. The results of the coupled models show that the agreement between the predicted permeability and that observed in the field is very good.

It should be noted that permeability was measured under hydrostatic conditions at laboratory where the confining pressure was equal in all directions and coal sample was allowed to expand to the confining fluid, whereas the models used to match the experimental data were derived for matchstick-type geometry under uniaxial strain conditions, assumed to describe field conditions more accurately. Thus the fracture was not closed as much as the models would expect. More importantly, most of the analytical models were developed assuming that the system reaches the equilibrium state, namely, the pressure in the fracture is equal to that in the matrix. Under the constant stress conditions at the laboratory, the permeability in coal should not change at the final steady state due to the uniform swelling of the coal sample or slightly increase due to the expansion of the coal matrix bridge which connects the coal matrix faces in the fracture. However, the laboratory observations are contradicted to all these predictions, suggesting that the current local equilibrium assumption based approach may not be appropriate because the equilibrium state might not have been achieved in the laboratory.

Even though laboratory measurements on coal core samples may be readily obtained, it is difficult to replicate reservoir conditions, particularly the stress state, at laboratory. When using laboratory measurements to test permeability models, differences in the boundary conditions and other assumptions have to be considered. In other words, the permeability model used needs to be appropriate for the test conditions. Models derived under conditions of uniaxial strain and constant vertical stress would not be appropriate for a laboratory test under constant stress conditions.

In previous studies (Liu et al., 2011b; Qu et al., 2012), the phenomenon of the permeability switch from reduction to rebound and the swelling transition from local to global swelling have been discussed under the stress controlled boundary condition. However, the driving mechanisms behind the distinct behavior of the permeability between the initial equilibrium state and the final equilibrium state have not been well studied. In this study, we extended previous research by developing the concept of matrix swelling area to define the relationship between matrix swelling transition and permeability evolution, and introducing a new concept of Critical Swelling Area to describe the dominant mechanism controlling the swelling transition and permeability switch.

In addition, the influence of external boundary on coal permeability was investigated. Two boundary conditions including the constant volume case (CVC) and the constant stress case (CSC) were applied to our model and the results of permeability evolution were compared. Moreover, the Thin Elastic Layer was simulated in the software of COMSOL as the coal bridge, partially connecting the matrix in the fracture, to account for the impact of matrix swelling on fracture aperture change. Furthermore, the impacts of initial matrix permeability and temperature on the propagation of the swelling area and permeability evolution were discussed as well.

The importance of this study is that we analyzed the matrix swelling propagation process under the constant stress boundary conditions by proposing the concept of Critical Swelling Area, which explains why permeability decreases at the early stage of gas injection and rebounds at a later stage. It rigorously couples the coal deformation process, as well as the gas flow and thermal transport processes in coal seams and underscores the impact of coal matrix swelling on the permeability change.

2. Conceptual model

Earlier research (Liu et al., 2011b) indicates that permeability switches from reduction to rebound during the injection of CO_2 due to the transition of coal matrix swelling from local swelling to global swelling. The matrix swelling processes control the evolution of coal permeability, which is determined by the matrix properties and can be described by the development of the matrix swelling area.

Fig. 1 illustrates the permeability evolution corresponding to the swelling propagation area. At the initial state, both the pressure in the coal matrix and that in the fracture are equal to the pressure in the reservoir. This is called the initial equilibrium state. At this stage, no gas is injected into the system and thus no swelling takes place. At the beginning of CO_2 injection, gas occupies the fracture only thus the pressure in the fracture increases almost instantly and reaches the same as the injection pressure while the pressure in the matrix remains zero.

There should be a quick increase in permeability after the gas injection due to the sudden increase of the fracture pressure. However, since it is assumed that gas occupies the fracture almost instantly, this permeability rise is ignored in our study and we focus mainly on the impact of coal matrix swelling on permeability.

With the increase of CO_2 injection, the pressure in the matrix increases slowly with the diffusion of the gas from the fracture to the matrix and the pressure difference between the fracture and the matrix reduces. At this stage, swelling only takes place in the fracture and the matrix in the vicinity of the fracture. Pressure in the matrix beyond this swelling area still remains zero because no gas has reached that area while the external boundary stays unmoved. This swelling stage is called the local swelling.

During the local swelling, the external boundary has no effect on permeability. On one hand, permeability in the fracture continuously declines due to the narrowing of the fracture aperture caused by the adsorption in the vicinity of the fracture. On the other hand, permeability increases due to the increase of pore pressure in matrix. However, the permeability increase is relatively small comparing to the permeability decrease since the pressure in the coal matrix is very low and increases slowly. At this stage, the permeability evolution is similar to the case of constant volume boundary since the area beyond the swelling area acts like shell wall and the total volume does not change.

As gas diffuses into the coal matrix far from the fracture, the pressure in the matrix increases accordingly and the area of matrix swelling induced by the gas sorption enlarges. As the swelling area extends to a certain area, the external boundary starts to move outwards due to the propagation of the matrix swelling. This certain swelling area is defined as the Critical Swelling Area. Beyond the Critical Swelling Area, the pressure in the matrix still remains zero or relatively low and the external boundary moves rigidly with the un-swelling matrix.

Critical Swelling Area is the area of coal matrix swelling at the permeability switching point when the external boundary starts to move outwards as the matrix swelling propagates to it. There are several characteristics indicating that the matrix swelling area reaches the Critical Swelling Area: 1) the external boundary starts to move outwards; 2) total volume/area of the coal model starts to increase; 3) permeability reaches the lowest point where it stops decreasing and starts to rebound. The Critical Matrix Area represents the area of matrix swelling at the lowest permeability point and can not be measured or calculated directly.

Coal matrix swelling is induced by gas adsorption, described by the modified Langmuir isotherms in this study. Sorption-induced

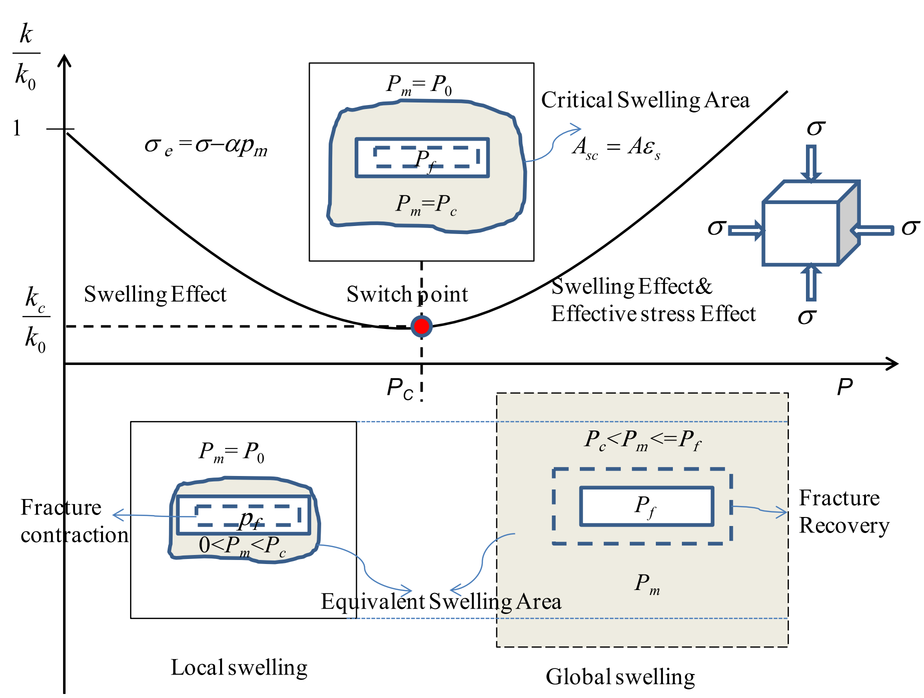

Fig. 1. Concept modeling of the swelling propagation area.

swelling is related to the sorption amount. According to the Langmuir isotherms, the sorption amount highly relies on the gas pressure and temperature in matrix and fracture. Since the pressure and temperature in fracture is assumed to reach the same as the injection value very soon, the sorption amount is determined by the gas pressure and temperature in matrix. On the other hand, the magnitude of the injection pressure and temperature affects the rate of gas flow in fracture and gas diffusion in matrix, determining the Critical Swelling Area at the permeability switch point. Therefore, the instantaneous matrix swelling area depends on the gas pressure and temperature in matrix while the Critical Swelling Area depends on the pressure and temperature of the injected gas.

The instantaneous matrix swelling area varies with the size of the model geometry. However, the matrix swelling area ratio rather than the instantaneous swelling area is concerned in this study. The swelling area ratio is defined as the ratio of the instantaneous swelling area to the total swelling area, and the instantaneous swelling area can be derived by the total area timing the swelling area ratio. The total area is calculated through the geometry size of the model during the local swelling stage. After the external boundary moves outwards, the total area of the model increases. Given the increase of the model area is relatively small comparing to the original size, the total area is assumed constant in the whole calculation. Since the instantaneous matrix swelling area can be calculated through the pressure in matrix, the swelling area ratio can be analogized to the matrix pressure ratio, namely, the ratio of instantaneous average matrix pressure to the injection pressure.

The Critical Swelling Area Ratio is the swelling area ratio at the permeability switch point, and is analogized to and calculated through the Critical Matrix Pressure Ratio, determined by the average matrix pressure at the permeability switch point over the gas injection pressure.

As the swelling area frontier passes the Critical Swelling Area, matrix swelling switches from local to global and the external boundary starts to affect permeability. Pressure in the rigid area increases slowly with gas diffusion, inducing the matrix around the external boundary to swell. Since the coal matrix is not completely separated but connected with the coal bridge, the swelling of the coal bridge in the fracture results in the increase of the fracture aperture and leads to permeability recovery. Meanwhile, with the increase of the pressure in the matrix, the effective stress decreases, resulting in the increase of permeability as well. At the final state, pressure in the matrix is equal to that in the fracture again and the same as the injection pressure. Gas sorption completes in both coal matrix and coal bridge and both fracture and matrix swell uniformly. Permeability in the fracture reaches equilibrium and may be higher than the initial permeability due to the swelling of the coal bridge.

The development of the swelling area and the effect of the sorption induced coal matrix swelling on the fracture permeability are controlled by the rate of gas diffusion and the amount of gas adsorption. Permeability decreases at the beginning because gas pressure in the matrix is very low; gas mainly adsorbs on the coal matrix in the vicinity of the fracture, narrowing the fracture aperture. The pressure in the coal matrix increases as the gas diffuses into the coal matrix, resulting in the increase in the area of the matrix swelling and the continuous reduction in permeability. Gas tends to adsorb on the coal surface at the early stage. However, as gas diffuses to the matrix far away from the fracture later and the pressure in the matrix reaches a proper value, the swelling of the coal matrix switches. Gas not only adsorbs on the coal surface, but also penetrates the coal matrix and absorbs inside the coal matrix.

The concept of the Critical Swelling Area was proposed in this study to quantify the swelling area development, which controls the switch of permeability from reduction to rebound corresponding to the transition of matrix swelling. The ratio of the Critical Swelling Area to the total area of the coal swelling was defined as the Critical Swelling Area Ratio. It relates the swelling area propagation to the pressure variation in the matrix, and discloses the critical relationship between the permeability evolution and the pressure distribution in the matrix at each specific matrix swelling area.

3. Quantification of Critical Swelling Area

The numerical models in this study were developed from the models we presented previously (Qu et al., 2012), which were based on the energy and mass conservation law, and coupled the conventional individual multiphysics (fluid flow, heat transfer and mechanical deformation). However, the previous model did not describe the coal bridge between the coal matrix.

Coal bridge has complex properties, determining permeability evolution during the CO_2 sequestration. However, it has not been well understood or investigated properly. We found that the Thin Elastic Layer has similar mechanical properties with the coal bridge in the fracture, and thus can be analogized to the coal bridge under proper assumptions.

In this study, we developed a new method to quantify the effect of matrix swelling on permeability evolution by applying the Thin Elastic Layer feature in the numerical software of COMSOL to take the coal bridge deformation into account in the study of fracture permeability change.

3.1. Effect of matrix swelling on permeability

Results from field and laboratory experiments indicate that coal permeability can change significantly during absorbable gas injection (e.g. CH_4 and CO_2). Permeability in the coal fracture can be defined through the fracture aperture and spacing as

$$k = \frac{b^3}{12s} \tag{1}$$

The initial fracture aperture can be derived as

$$b_0 = \sqrt[3]{12sk_0} \tag{2}$$

where b_0 is the initial fracture aperture, s is the fracture spacing in the horizontal plane, and k_0 is the initial fracture permeability.

The dynamic permeability in the fractured coal system is expressed through the cubic law as

$$\frac{k}{k_0} = \left(1 + \frac{\Delta b}{b_0}\right)^3 \tag{3}$$

where Δb is the change in the fracture aperture, which is controlled by the sorption induced swelling, thermal expansion and the effective stress variation.

3D model was developed in this study. To derive the analytical solution for the permeability in the fracture, we assume the geometry of the fracture system contains the fracture height, w in the vertical direction.

The total volume of the fracture, V, is defined as (Izadi et al., 2011)

$$V = s^3 \tag{4}$$

According to the definition of the effective strain, the volume change of the system ΔV caused by the sorption induced swelling, thermal expansion and effective stress is defined as

$$\Delta V = V \cdot \varepsilon_e \tag{5}$$

where ε_e is the effective strain, and can be defined as

$$\varepsilon_e = \varepsilon_v - \varepsilon_s - \varepsilon_T + \frac{p_m}{K_m} \tag{6}$$

where ε_v is the total volumetric strain, developed from the stress–strain relationship, ε_s is the sorption induced strain, ε_T is the thermal strain, p_m is the pressure in the matrix, and K_m is the bulk modulus in the coal matrix.

Assuming that the coal deformation only applies on the fracture aperture while the fracture height and fracture spacing remains constant, the volume change of the fracture aperture during the gas injection ΔV_f is calculated as

$$\Delta V_f = s \cdot w \cdot \Delta b \tag{7}$$

Under the constant volume condition, the displacement on the external boundary is zero, namely, $\varepsilon_v = 0$. The total volume change of the coal matrix caused by the effective strain should be equal to the volume change in the fracture. That is,

$$\Delta V = \Delta V_f \tag{8}$$

Substituting Eqs. (4), (5) and (7) into Eq. (8), the change in the fracture aperture can be derived as

$$\Delta b = \frac{s^2 \varepsilon_e}{w} \tag{9}$$

and

$$\frac{\Delta b}{b_0} = \frac{s^2 \varepsilon_e}{w b_0} \tag{10}$$

Substituting Eq. (10) and the effective strain Eq. (6) into Eq. (3), the permeability ratio in the fracture can be expressed as

$$\frac{k}{k_0} = \left(1 + \frac{s^2 \varepsilon_e}{w b_0}\right)^3 \tag{11}$$

$$\frac{k}{k_0} = \left(1 + \frac{s^2}{w b_0}\left(\varepsilon_v - \varepsilon_L\left(\frac{p_m}{p_m + p_L} - \frac{p_0}{p_0 + p_L}\right) - \alpha_T (T - T_0) + \frac{p_m - p_0}{K_m}\right)\right)^3 \tag{12}$$

where p_m is the pressure in the matrix, p_0 is the initial pressure, p_L is the Langmuir pressure, ε_L is the maximum swelling strain, T_0 is the initial temperature and α_T is the thermal expansion coefficient. Under the constant volume condition, the pressure in the matrix at the steady state is the same as that in the fracture, and the analytical solution for the fracture permeability can be calculated from the above equation.

$$\text{Assuming } \frac{s^2}{w b_0} = \gamma, \tag{13}$$

permeability is then derived as

$$\frac{k}{k_0} = (1 + \gamma \varepsilon_e)^3 \tag{14}$$

where γ is named as the coefficient of effective strain.

Under the constant stress condition, permeability experiences a 2-stage evolution, decreasing at the beginning and recovering at a later stage. At the local swelling stage, the total volume of the coal does not change. Permeability declines due to the swelling of the matrix in the vicinity of the matrix, which can be expressed in the same way as that in the constant volume case as

$$\frac{k}{k_0} = \left(1 + \gamma\left(-\varepsilon_L\left(\frac{p_{mc}}{p_{mc} + p_L} - \frac{p_0}{p_0 + p_L}\right) - \alpha (T - T_0) + \frac{p_{mc} - p_0}{K_m}\right)\right)^3 \tag{15}$$

where p_{mc} is the pressure in the matrix at the permeability switching point, which controls the matrix swelling transition.

As the external boundary starts to move outwards, the total volume of the coal increases with the swelling of the matrix. At the equilibrium time, the pressure in the matrix is the same as that in the fracture and equal to the injection pressure. Permeability is still determined by the sorption induced swelling, thermal expansion and effective stress variation, but the proportion and magnitude of the effective strain in determining permeability would be different, which can be described by a different coefficient in front of the effective strain. The permeability at the global swelling stage is expressed as

$$\frac{k}{k_0} = \left(1 + \beta\left(\varepsilon_v - \varepsilon_L\left(\frac{p_{inj}}{p_{inj} + p_L} - \frac{p_0}{p_0 + p_L}\right) - \alpha (T_{inj} - T_0) + \frac{p_{inj} - p_0}{K_m}\right)\right)^3 \tag{16}$$

where β is the coefficient of the effective stress under the constant stress boundary condition, p_{inj} is the injection pressure and T_{inj} is the injection temperature. Therefore, the permeability change in the fracture under the constant stress condition is determined by the development of the swelling area of the matrix and can be quantified piecewise through the different expression of the coefficients γ and β in front of the effective strain as

$$\frac{k}{k_0} = \left\{ \begin{array}{ll} (1 + \gamma \varepsilon_e)^3, & k \ll k_c \\ (1 + \beta \varepsilon_e)^3, & k > k_c \end{array} \right\} \tag{17}$$

where k_c is the fracture permeability at the switching point. γ is dependent on the property of the fracture during the permeability reduction while β is determined by the property of the coal bridge because permeability at the steady state is controlled by the swelling of the coal bridge as a result of the gas adsorption and thermal expansion under the constant stress condition.

3.2. Simulation on swelling of the coal bridge through the Thin Elastic Layer

Coal is normally interpreted as a dual porosity medium characterized by two distinct pore systems, micro pores and macro pores. The micro pores are contained in the coal matrix and are the main space for gas storage while the macro system is normally described as networks of fractures, which are called cleats, providing dominant flow paths for the fluid. Permeability in coal normally refers to the permeability in fracture, which can be significantly affected by the matrix swelling during CO_2 sequestration due to the large adsorption capacity of coal for CO_2.

Coal permeability was analyzed through the interactions between the coal matrix and fracture. Fractures do not create a full separation between adjacent matrix blocks, but solid rock bridges are present. The sorption-induced swelling strain is accommodated over two components, the contacting coal bridges that hold fracture faces apart and the non-contacting span between these bridges. The effects of swelling act competitively over these two components. At final equilibrium stage, both the coal bridges and the coal matrix swell, and permeability depends on the property of coal bridge. As a result, the swelling of the contacting bridges enlarges the fracture aperture and increases permeability while permeability decreases where matrix is separated completely due to the closure of the fracture aperture caused by the swelling of the intervening matrix-faces.

The impact of the matrix–fracture interactions in coal on permeability evolution has not been incorporated appropriately (Izadi et al., 2011; Liu and Rutqvist, 2010) because the influence of the coal bridge swelling has not been taken into account or quantified in large scale due to the small size of the fracture in coal.

In our numerical simulation, permeability and the mechanical deformation in the fracture was simulated by the fracture aperture change through the Thin Elastic Layer. The Thin Elastic Layer feature represents the fracture, which is normally interpreted as the interior boundary in the coal sample. Face a and face b represent the two faces of the fracture, as shown in Fig. 2. The Thin Elastic Layer feature connects two faces of the fracture like a spring with both elastic and damping boundary conditions. The change in permeability can be simulated through the difference of the displacements of these two faces.

On the other hand, the Thin Elastic Layer is analogous to the coal bridge and used to simulate the geomechanical deformation in the fracture and swelling caused by the coal bridge. In coal samples, coal bridges partially occupy the fracture and apply forces to the coal matrix. The forces that the Thin Elastic Layer provides the matrix with can also be similarly calculated by the displacements difference between two connecting faces.

The deformation of the coal bridge was simulated through the spring constant k_s in this study, assuming that the forces generated by the coal bridge are identified with those generated by the thin elastic layer.

The volumetric strain–stress relationship of the coal bridge can be defined as:

$$\Delta\varepsilon_{vb}K = 3\frac{\Delta l_b}{l_b}K = \sigma_{vb} = \frac{3F_b}{A_b} \quad (18)$$

where $\Delta\varepsilon_{vb}$ is the volumetric strain of the coal bridge, Δl_b is the displacement of the coal bridge, l_b is initial fracture aperture, K is the bulk modulus, σ_{vb} is the volumetric stress of the coal bridge, A_b is the connecting area between the coal bridge and the matrix surface and F_b is the force generated by the coal bridge, which can be derived as

$$F_b = KA_b\frac{\Delta l_b}{l_b} \quad (19)$$

The force generated by the thin elastic layer is expressed as:

$$F_e = P_eA_e = k_suA_e \quad (20)$$

where F_e is the force generated by the thin elastic layer, P_e is the pressure applied by the thin elastic layer, u is the displacement difference between two connecting faces of the fracture and A_e is the area of the fracture.

According to the assumption, $u = \Delta l_b$ and $F_b = F_e$, applying the two equations into Eq. (19) and Eq. (20), the spring constant k_s can be derived as:

$$k_s = \frac{KA_b}{l_bA_e} \quad (21)$$

Given that the bridges only occupy a fraction of the fracture and the connecting area of the coal bridges with the coal matrix is small, we apply $A_b/A_e = 1/100$ in Eq. (21) in our simulation.

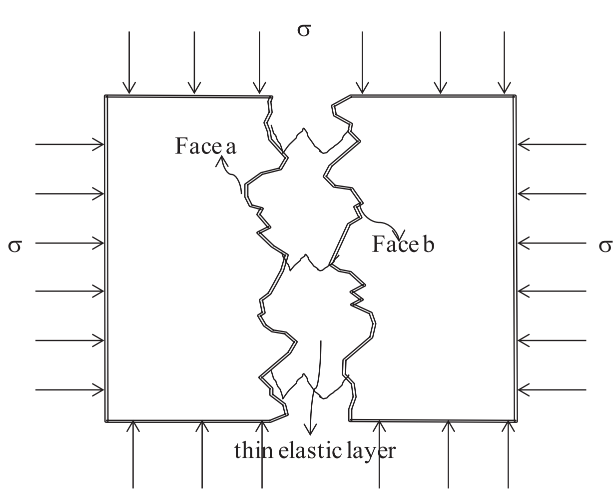

Fig. 2. Configuration of the Thin Elastic Layer in coal.

4. Simulation modeling

In this section, a series of numerical tests were conducted to evaluate the complex evolution of coal permeability under different boundary conditions during CO_2 injection. The numerical model coupled with multi-physics of mechanical deformation, gas flow and transport as well as thermal conservation was solved in the software of COMSOL Multiphysics. The concept of swelling area was incorporated in the numerical model through the sorption-induced swelling (Qu et al., 2012). Thin Elastic Layer is applied in the software to simulate the swelling of coal bridge for the study of the fracture permeability.

Two extreme cases, Constant Volume Case (CVC) and Constant Stress Case (CSC) were investigated in the 3D non-isothermal CO_2 injection scenarios and the concept of the Critical Swelling Area was applied to analyze the results in the CSC.

In the CVC, the internal constraint is coincident with the external one. The whole system behaves as a constant volume all the time, while in the CSC, the internal constraint is not coincident with the external one. The whole system experiences a transition from CVC to CSC. Analytical solutions were developed under the equilibrium conditions and the numerical modeling was verified by matching the numerical results with the analytical solutions. We then applied the numerical modeling to investigate the development of the Critical Swelling Area.

The geometry is defined as a cylinder with the height of 0.1 m and the radius of 0.025 m. One single fracture crosses the central axis and penetrates the cylinder in the axial direction, as shown in Fig. 3. Point A at (0, 1) is an observation point for the strain analysis in Section 5.4. No flow and no thermal insulation are applied on the boundary in each direction. No fluid or heat flux flows through any boundary but velocity and temperature are allowed to change. A uniform CO_2 injection pressure of 10 MPa is applied in the fracture embedded within the coal solid where the initial pressure is 0.1 MPa. The temperature of injected CO_2 is 328.15 K while the initial temperature in the coal seams remains at 298.15 K.

In the software of COMSOL simulation study, only one condition (either stress or strain) can be applied on each boundary. Constant stress is applied to each boundary in the Constant Stress Case while constrained boundary condition is applied to each boundary in the Constant Volume Case. Displacement of the external boundary was

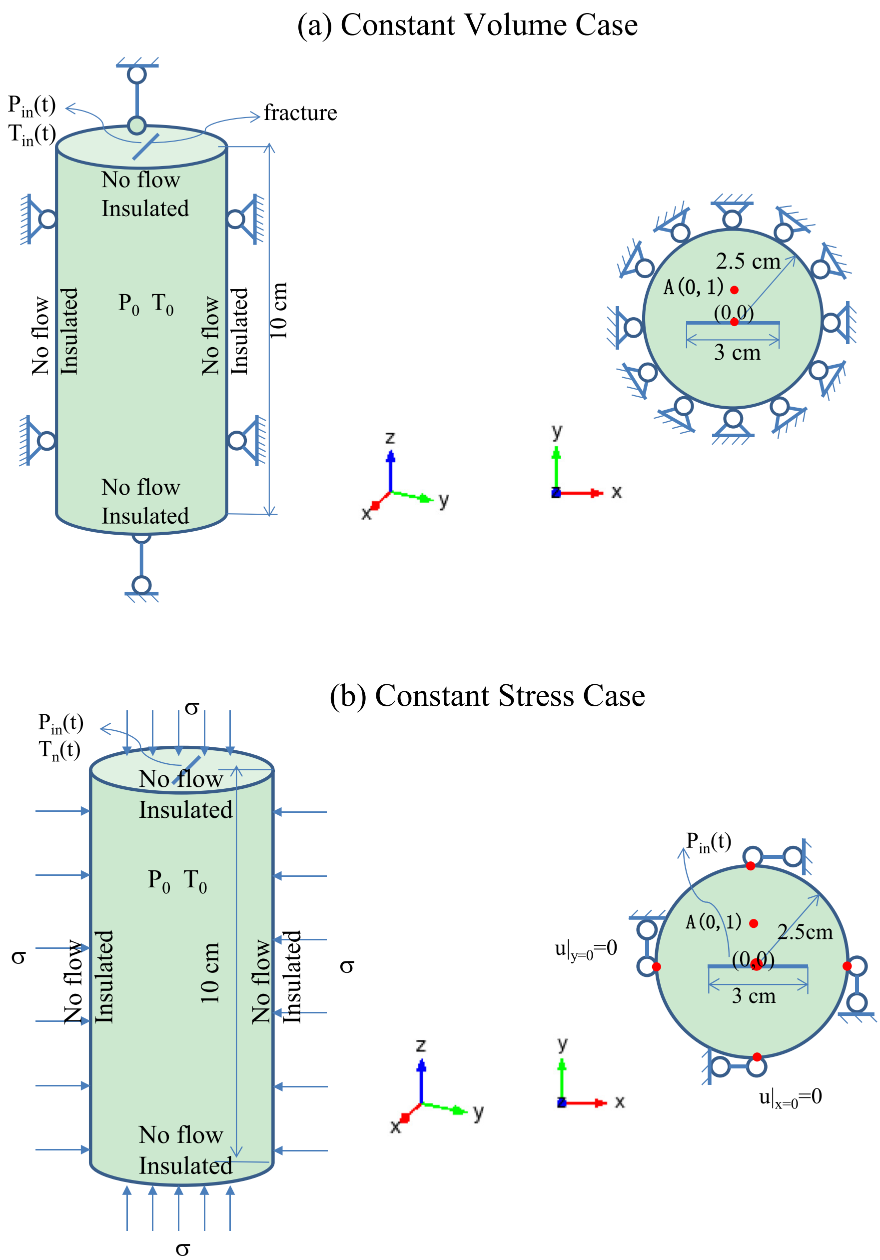

Fig. 3. Geometry of the numerical models under two boundary conditions.

fixed in the Constant Volume Case and no stress is applied. Fig. 3 (a) presents the Constant Volume Case where all external surfaces are constrained. Fig. 3 (b) shows the Constant Stress Case, where constant total stress is applied on the external boundary that is free to deform. Material properties applied to the model are detailed in Table 1.

5. Results and discussions

It was assumed that the thermal equilibrium between injected CO_2 and coal is not reached instantly in our simulation. The 3D simulation results from our numerical model under the constant stress boundary condition were matched with the theoretical solutions. Permeability evolutions were studied in the CVC and CSV, respectively, through the development of matrix swelling area, to investigate the impact of the boundary conditions on fracture permeability.

All the simulations in this study were conducted from three aspects. The fracture aperture change was simulated through dynamic interactions between coal matrix swelling/shrinking and fracture aperture alteration, and these interactions were translated to permeability evolution under each boundary condition. Then the concept of the swelling area was applied to the swelling process and permeability evolution response to the swelling area propagation was investigated. Lastly, the effect of initial matrix permeability and temperature on the permeability evolution and swelling area propagation was examined.

5.1. Model validation

Assuming experiments were conducted under completely constrained conditions, the bulk volume of a coal sample would not change during the experiment. Under this assumption, 100% of coal swelling would contribute to the reduction of coal permeability.

Table 1
Parameters input in the simulation cases.

Parameter	Value
Porosity (%)	5
Matrix permeability (m^2)	10^{-22}
Gas viscosity (Pa * s)	1.2278×10^{-5}
Young's modulus (GPa)	3.95
Poisson ratio	0.339
Biot's coefficient	0.66
Thermal expansion coefficient	9×10^{-5}
Coal density (kg/m^3)	1500
Langmuir strain	0.03
Langmuir volume (m^3/kg)	0.04316
Langmuir pressure p_L (MPa)	3.96
Confining pressure (MPa)	12
Initial Temperature (K)	298.15
Universal gas constant (m^3 Pa/(mol K))	8.3144
Reservoir pressure (MPa)	0.1
Fracture spacing (m)	0.01
Fracture aperture (m)	0.0001

This represents the Constant Volumetric Case. However, most laboratory experiments have been conducted under the conditions of constant stress. The experimental results are supposed to be equal to or at least close to the theoretical solution under these constant stress conditions. In other words, permeability should increase with the injection of CO_2 due to the uniform swelling of both coal matrix and fractures, as shown in Fig. 4. Nevertheless, experimental results are inconsistent with the theoretical analysis. For instance, dramatic reduction was shown in permeability with the injection of an adsorbing gas (Harpalani and Chen, 1997; Pan et al., 2010; Pini et al., 2009). These results were close to the solution in the constant volumetric case even though they were made under the condition of constant stress.

Two reasons may account for this inconsistent phenomenon. Firstly, although constant stress was applied to the coal sample in the lab experiments, the experimental results were normally interpreted by using permeability models under the assumptions of uniaxial strain, resulting in an inconsistency between the experimental and modeling conditions.

Secondly and more importantly, this discrepancy is probably due to the constraint of experiment conditions. Permeability should be measured after the gas adsorption reaches equilibrium. When CO_2 is injected into the coal seams, gas diffuses from the fractures to the matrix before it adsorbs on the surface of the pores. Since the process of the gas diffusion in the coal matrix is very long, the experiment data may have often been collected before the gas diffusion and gas adsorption reach equilibrium. As a result, the matrix swelling may be still localized in the vicinity of the fracture compartment and has not changed to the global swelling. Consequently, no permeability switch or only a little permeability rebound has been observed in the laboratory under some experiment conditions. Apart from these two reasons, there could be other reasons causing the inconsistency between the experiment results and theoretical solutions, which needs to be further investigated.

In all modeling examples, permeability at the initial and final state conditions is known. The numerical solutions from our simulation for permeability at different pressures were compared with the theoretical solutions in Fig. 4. The numerical solutions virtually match the theoretical solutions, indicating the validity of the numerical modeling approach.

5.2. Permeability evolutions under two boundary conditions

The evolution of permeability ratio over time at the temperature of 328.15 K is compared under two boundary conditions in Fig. 5, indicating that boundary conditions significantly affect the trend of permeability evolution, the time of the permeability evolution and the magnitude of the permeability change.

Permeability shows distinctive patterns under these two boundary conditions. The constant volume boundary condition produces a decrease in permeability ratio with no sign of permeability recovery. Permeability ratio decreases from 1 to 0.91 in the first 5×10^3 s, followed by a steep decline to 0.09 between 5×10^3 s and 2×10^5 s, with the permeability ratio stabilizing at around 0.07 after 3×10^5 s. In contrast, under the constant stress condition, permeability decreases at the beginning, but then recovers to a level of permeability slightly over the initial permeability. Specifically, permeability ratio declines gradually from 1 to 0.64 in the first 7×10^4 s and then recovers to just over 1, reaching the equilibrium state after 5×10^5 s.

Under the constant volume boundary condition, permeability keeps decreasing and does not produce any recovery because the swelling of the coal matrix contracts the fracture and narrows the fracture aperture all the time due to the constraint of the external boundary conditions. The external boundary surface is constrained in both x and y directions and could not move as the matrix swelling propagates to the boundary. The fracture, therefore, is kept

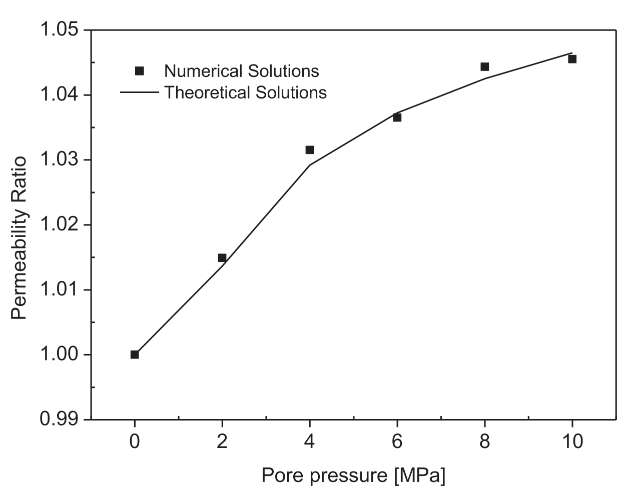

Fig. 4. Match of the theoretical solutions with the numerical solutions for the CSC.

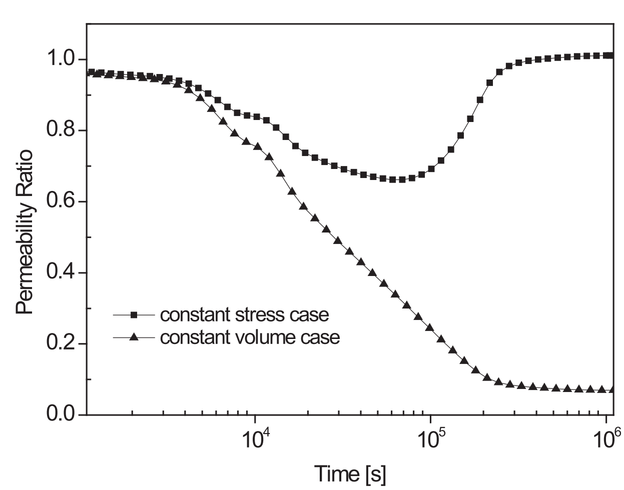

Fig. 5. Evolutions of permeability ratio with time under two boundary conditions.

compacted until the pressure in the whole coal matrix reaches the steady state.

Under the constant stress boundary condition, on the contrary, there is a permeability rebound after the permeability reduction because the external boundary in the *y* direction is allowed to move as the swelling of the matrix reaches the external boundary. The free swelling of the coal matrix stops the fracture from being compressed due to the swelling of the matrix in the vicinity of the fracture. The fracture aperture, therefore, widens again and the permeability rebounds. The time of the transition in permeability corresponds to a specific swelling area of the coal matrix. The concept of the swelling area is proposed in this study to further interpret the reason behind the permeability evolution. The relationship between permeability and the matrix swelling area is discussed in Section 5.5.

The results also show that the recovery process of permeability is much slower than the reduction process under the constant stress condition. It takes about 9 times longer for permeability to recover, as shown in Fig. 5, suggesting that the global swelling should be much slower than the local swelling. It is speculated that the critical area ratio should be less than 50% at the permeability switch point because the swelling area at the local swelling stage is likely to be smaller than that at the global swelling stage given the time difference in permeability evolution.

The magnitude of permeability reduction is fairly different in these two cases. It is obvious that the permeability decrease under the constant stress boundary condition is only 10%–40% of that under the constant volume boundary condition. The less permeability reduction in the first case is due to the switch in the matrix swelling, which eases the compact of the fracture and stops the permeability from further decreasing. However, permeability reaches the equilibrium almost at the same time under the two boundary conditions since the equilibrium time is determined by the gas adsorption and gas diffusion process which is controlled by the injection pressure and the initial matrix permeability. The effect of the initial matrix permeability on the fracture permeability evolution is discussed in Section 5.6.

5.3. *Evolutions of the displacement profile in the x–y plane cross-section of the coal sample*

Fig. 6 illustrates the displacements of the fracture and the volumetric change of the coal sample in the down half geometry of the *x*–*y* plane cross-section under two boundary conditions at three specific times during the period from the initial condition to the equilibrium state with the injection of CO_2. The up half geometry has similar changing trend of displacement due to the symmetry of the model geometry. It indicates the path in which the coal sample expands and the magnitude of the expansion in each direction in the *x*–*y* plane due to the adsorption of CO_2.

Noticeably, in the case of the constant stress boundary condition, coal matrix swells in *x* and *y* directions and fracture aperture becomes narrower due to the swelling of the fracture surface caused by gas adsorption. There are 2 stages of fracture face movements. In the early stage, the down face of the fracture moves up and the up face of the fracture moves down, narrowing the fracture and reducing the fracture aperture. In the late stage, the down face of the fracture moves down and the up face of the fracture moves up, widening the fracture and increasing the fracture aperture. The change in fracture aperture is the key reason for fracture permeability change. Therefore, permeability decreases at the early stage and rebounds later. Specifically, the displacement of the fracture and the volume of the coal mass increase considerably before 10^5 s. Then the total volume continues to increase but the displacement of the fracture in the *y* direction decreases till 10^8 s.

In contrast, under the constant volume boundary condition, distinct phenomenon was shown in terms of the displacement of the fracture and the total volumetric change. There is no change in the bulk volume of the coal mass because the external boundary was fully constrained and not allowed to move in any direction. However, displacement in the fracture is quite substantial. Significant displacement in the fracture was obtained in *y* direction, which increases with time and reaches the maximum as the matrix swelling gets equilibrium.

The external boundary conditions have an important impact on the change in the displacement of the fracture and the volume of the coal mass, by controlling the matrix swelling switch. The free swelling external boundary under the constant stress condition determines the switch of the fracture displacement from increase to decrease and the continuous increase in the total volume of the coal mass. The displacement of the fracture increases at the local swelling stage with the increase of the sorption-induced strain due to the CO_2 adsorption on the matrix in the vicinity of the fracture. As the swelling switches from local swelling to global swelling, the external boundary moves outwards, leading to an increase of the total volume. Meanwhile, the free swelling of the external boundary releases the tension in the fracture, reopening the fracture and reducing the fracture displacement. The displacement evolution of the fracture under these two different boundary conditions explains the permeability evolutions in Fig. 5 and further supports the method we applied in this study of calculating permeability through the change in fracture aperture.

5.4. *Effect of the components of the effective strain on the evolution of permeability*

The fracture permeability is calculated according to the change in the fracture aperture, which is not caused by the deformation of the fracture itself but affected by the matrix swelling. In fact,

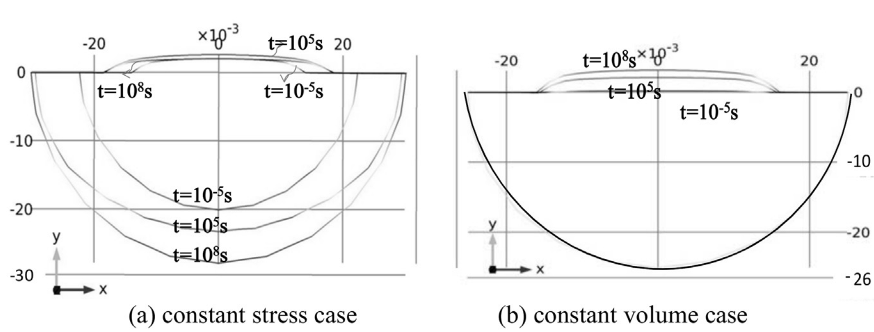

Fig. 6. Displacement profiles of the *x*–*y* plane under two boundary conditions.

permeability evolution in the fracture is a reflection of the matrix swelling process, which is determined by the effective strain in the matrix.

Figs. 7 and 8 compare the evolution of each component of effective strain at the observation point A (0, 1) in the matrix during the CO_2 injection under the constant stress and constant volume boundary conditions.

Under the constant stress boundary condition, the magnitude of the effective strain increases rapidly to 1.8% in the first 10^4 s then decreases slightly later and stabilizes at 1.6% after 2×10^5 s, as shown in Fig. 7. In the case of the constant volume boundary condition, the magnitude of effective strain keeps increasing to 1.9% at 10^4 s and reaches steady state at 1.98% after 2×10^5 s as well, as shown in Fig. 8.

The sorption-induced strain, thermal strain and the strain caused by solid compression follow similar changing trends and reach similar values in these two cases. In each case, the sorption-induced strain changes considerably by 2% while the thermal strain and the compressibility strain change by 0.25%. However, the total volumetric strain behaves differently under the two boundary conditions. Under the constant stress boundary condition, the total volumetric strain is negative 0.25% at the beginning, indicating the matrix is compacted due to the existence of the initial stress and the displacement of Point A therefore is negative. It increases gradually in the first 10^4 s until the value grows positive and then increases with a relatively constant increasing rate and reaches equilibrium at around 3×10^5 s. In the case of constant volume, however, each initial strain component is zero since there is no stress applied. The total volumetric strain increases slowly in the first 10^4 s to 0.3% but then decreases a little to 0.2% and remains stabilized after 3×10^5 s.

The phenomenon of total volumetric strain increasing first and decreasing later in the Constant Volume Case can be explained by the theory of ‘free expansion & pushing back’ (Liu et al., 2011c). As the matrix swelling propagates from the fracture to Point A, it moves towards the external boundary and the total volumetric strain at this point increases. However, since the total volume of the whole sample is constant and the external boundary can not move, Point A is pushed back a little as the matrix swelling near the external boundary propagates oppositely to Point A, and the total volumetric strain at this point decreases accordingly.

The effective strain is a combined effect of total volumetric strain, sorption-induced strain, compression strain and thermal strain. The increase of the total volumetric strain and the strain

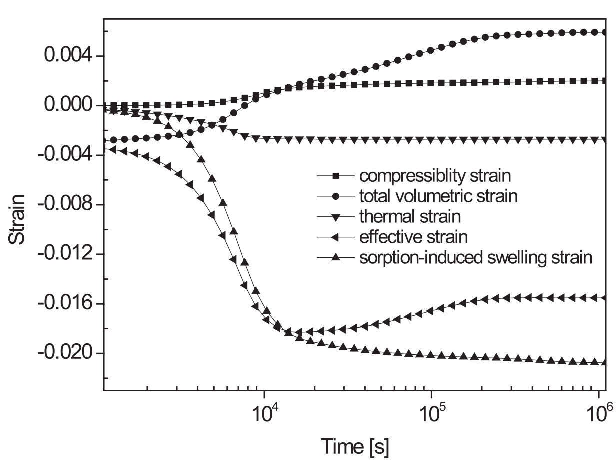

Fig. 7. Evolution of each component in effective strain at Point A in the matrix at 328.15 K under the constant stress boundary condition.

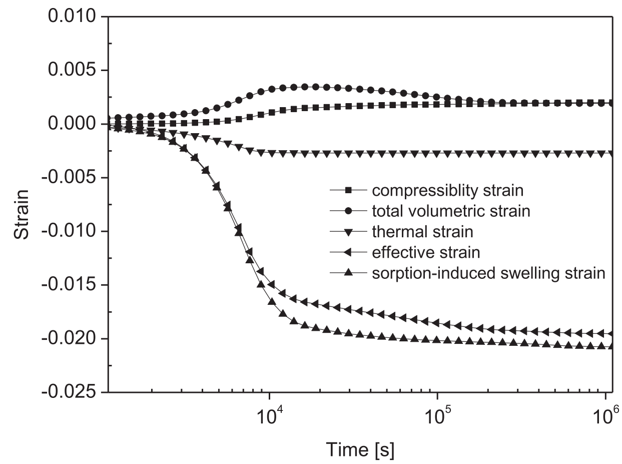

Fig. 8. Evolution of each component in effective strain at Point A in the matrix at 328.15 K under the constant volume boundary condition.

caused by the compression of coal grain has positive effects on permeability and keeps it increasing. The sorption-induced strain and temperature-increase induced thermal strain, however, lead to the expansion of the coal matrix, narrowing the fracture aperture and reducing permeability. These strains do not have constant and equal effect on permeability during the whole process and in fact, they affect permeability at different stages and to different extents during the CO_2 injection. Heat transfer, for instance, reaches equilibrium in a relatively short time and then the thermal strain remains stable while the other three strains continue to change and affect the permeability evolution. Particularly, the sorption induced strain changes dramatically and dominates the effective strain and permeability change from the beginning to the end. The total volumetric strain is another important cause of the change in the effective strain, but the magnitude is relatively small.

The effective strain is affected by the internal and external boundary simultaneously. The internal boundary refers to the fracture. The external boundary refers to the boundary of the whole sample where constant stress or constant volume boundary condition is applied in this study. The swelling strain responds to the internal boundary while the total volumetric strain responds to the external boundary. On one hand, the sorption-induced swelling strain dominates the change in the effective strain. The internal boundary is compressed due to the swelling of the coal matrix, leading to an increase in the swelling strain. On the other hand, the total volumetric strain determines the difference in effective strain evolution with time in Figs. 7 and 8 since the thermal strain, the swelling strain and the compressibility strain almost show the same trend in both figures.

The misidentification in the total volumetric strain in Figs. 7 and 8 is caused by the difference of the external boundary conditions. The continuous increase in the total volumetric strain reveals the free moving external boundary in the CSC while the decrease at the later stage discloses the constraint of the external boundary condition in the CVC. Under the constant volume condition, the total volumetric strain increases at the beginning is due to the sorption-induced matrix swelling. However, since the external boundary is fully constrained, the volumetric strain decreases as the swelling propagates to the external boundary. In contrast, under the constant stress condition, the volumetric strain increases at the beginning during the local matrix swelling stage. As the swelling propagates to the external boundary, the external boundary is allowed to move freely, resulting in a continuous increase in the total volumetric strain.

The strain components evolution in Figs. 7 and 8 explains the displacement evolution of the fracture in Fig. 6 and the permeability evolution in Fig. 5 because permeability is determined by the effective strain. The decrease in the effective strain at the beginning and the rebound at the later stage under the constant stress boundary condition caused by the continuous increase in the total volumetric strain due to the free swelling external boundary condition, as shown in Fig. 7, results in a decrease in the permeability followed by a recovery. However, permeability keeps decreasing under the constant volume condition because the effective strain in Fig. 8 continues to decline all the time caused by the decrease in the total volumetric strain due to the constrained external boundary.

5.5. *Effect of the matrix swelling on the evolution of permeability*

The concept of the Critical Swelling Area was proposed in this study to describe the condition of the permeability switch under the constant stress condition. As the swelling of the matrix propagates beyond the Critical Swelling Area, the matrix and the fracture swell globally. Since the fracture only separates the matrix blocks but does not cut through the whole matrix completely, the swelling of the coal bridges due to the CO_2 adsorption tends to reopen the fracture until the fracture aperture grows over the initial aperture when it reaches the steady state, leading to a permeability ratio of over 1.

The way of the coal matrix swelling changes from local swelling to global swelling when the average pressure in the matrix reaches the critical value as gas diffuses to the matrix relatively far away from the fracture. The Critical Swelling Area, used to localize the switching point in the fracture permeability evolution, corresponds to the area where the average pressure in the matrix reaches the critical pressure.

Since the time at the switching point could be easily monitored, the Critical Swelling Area could be simulated at the transition point and the Critical Swelling Area ratio could be calculated approximately by the ratio of the average pressure in the coal matrix at the switching point to the final pressure in the matrix at the steady state. The Critical Swelling Area ratio is used as an indicator of the permeability switch because both the Critical Swelling Area and the critical pressure represent the condition of the permeability switch.

Permeability ratio and the matrix swelling area ratio as well as the average pore pressure ratio in the coal matrix evolution were plotted with time in Fig. 9. The swelling area ratio and the average pressure ratio in the coal matrix increase continually while permeability switches from reduction to rebound under the constant stress condition. The increasing rate of the swelling area ratio and the average pore pressure ratio is relatively small during the permeability reduction compared to the large increasing rate during the permeability recovery.

Both the local swelling area ratio and the average pressure ratio increase slowly to 0.1 in the first 10^4 s. At this stage, permeability ratio decreases gradually with the increase of the swelling area to around 0.85. After 10^4 s, the swelling area ratio and the average pressure ratio increase at constant rates to 0.45 and 0.28 respectively, while permeability decreases sharply and reaches the lowest point of 0.7 at 7×10^4 s when local swelling switches to global swelling and permeability starts to recover. After the switching point, the swelling area ratio, the average pressure ratio, and permeability go up rapidly until they reach equilibrium.

The change in permeability is primarily caused by the sorption induced swelling with the increase of the pore pressure in the coal matrix. As CO_2 is injected into the coal, it diffuses from the fracture into the coal matrix and adsorbs on the coal surface. At the beginning, CO_2 only adsorbs in the vicinity of the fracture, resulting in the local swelling of the coal matrix. The sorption induced matrix

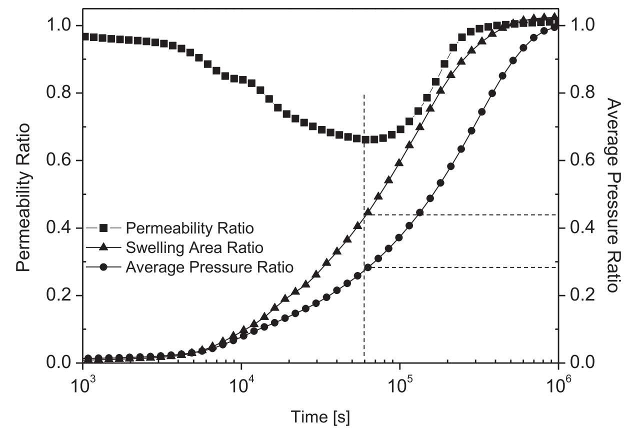

Fig. 9. Permeability ratio, swelling area ratio and average pressure ratio evolution with time for CSC at 328.15 K.

swelling narrows the fracture aperture and decreases permeability. As gas diffuses further into the coal matrix, the area of the coal matrix swelling increases and the fracture aperture continues to decrease until the swelling switches when the permeability stops decreasing and begins to rebound.

Permeability is affected by the external boundary condition as well. During the local swelling, the total volume of the coal does not change. Permeability decreases continually as it does under the constant volume condition, and the swelling area continues to increase in a local scale. The area beyond the local swelling area can be considered as a rigid shell and acts the same as the external boundary. During the global matrix swelling however, both matrix and fracture swell together. As a result, the total volume of the coal increases and the fracture stops being compressed and starts to reopen again, thus permeability stops decreasing and starts to rebound. The coal mass swells uniformly until the equilibrium is reached.

The matrix swelling area at the permeability switching point is presented as the Critical Swelling Area (CSA), referring to the critical point where the swelling switches. The Critical Swelling Area is very important to interpret the process of permeability evolution and the mechanism for permeability rebound. In this case, the Critical Swelling Area is 0.44 while the permeability is 0.68.

The scenario of permeability recovery was discussed in another paper (Izadi et al., 2011), where the initial permeability reduction was attributed to the swelling of the unconstrained block, and the subsequent recovery was believed to be caused by the effective stress given the swelling effects halt at high pressure. According to their conclusion, the pore pressure should have virtually reached the equilibrium before the permeability recovery and thus the swelling area should have occupied the whole area of coal. However, it is not the case as shown in our study.

Fig. 9 illustrates that at the permeability switch point, the swelling area of the coal matrix is less than 50%, and the average pore pressure in the coal matrix is still very small, less than 30% of the injection pressure, suggesting that the swelling effect should still be increasing as well as the pore pressure. Consequently, the effective stress should not be the sole reason causing the permeability to rebound at the later stage. The swelling effect, on the contrary, is mainly responsible for the fracture aperture widening due to the free moving of the external boundary under the constant stress condition.

Under the constant stress condition, the external boundary is allowed to move with the swelling of the coal matrix during the global swelling. As a result, permeability starts to increase due to the swelling of the coal matrix bridge in the fracture. Meanwhile, the increase of the pore pressure leads to the reduction of the effective stress, resulting in the increase in permeability. However, the decrease of the effective stress is only part of the reason for the increase in permeability. More importantly, the swelling of the coal bridge connecting the walls of the fracture enlarges the fracture aperture and permeability finally grows over the initial permeability when both the coal bridge and coal matrix reach the equilibrium state.

The corresponding relationship between permeability and the swelling area evolution discloses the mechanisms of gas diffusion and gas adsorption in the coal matrix and also reveals the transition between gas adsorption and gas absorption during the CO_2 sequestration. The process of permeability evolution and gas adsorption affects each other. On one hand, gas adsorption induces coal matrix swelling and affects the permeability. On the other hand, permeability affects the rate of the gas diffusion and gas adsorption.

The swelling area increases slowly at the beginning because permeability decreases at the local swelling stage; thus the gas diffusion rate in the matrix declines, resulting in a slow increase in the gas adsorption. In other words, the area of the coal matrix swelling increases with the increase of the gas adsorption while the rate of the swelling propagation decreases due to the reduction of the permeability. The equivalent Critical Swelling Area at the permeability switch point only accounts for 45% of the total area because practically most of the gas adsorbs on the coal surface at the local swelling stage and only a little gas permeates the coal matrix to absorb inside the coal matrix. This result verifies our speculation in section 5.1. The matrix swelling is mainly caused by the surface swelling at this stage.

After the matrix swelling switches, permeability starts to rebound and the gas diffusion rate increases accordingly. As a result, the swelling area propagates faster at the global swelling stage than at the local swelling stage, which accounts for the larger increasing rate for the swelling area ratio and the average pressure ratio in the matrix. With the increase of the swelling area and the matrix pressure, gas not only adsorbs on the coal surface, but more gas permeates the coal matrix, diffusing into the inside of the coal matrix and absorbing in the coal until the whole system reaches equilibrium. The amount of gas adsorption increases rapidly with the increase of the pressure in the matrix. At the global swelling stage, both gas adsorption and gas absorption occur. The coal swelling is attributed to the surface swelling caused by the gas adsorption and the volume swelling due to the gas absorption.

Therefore, from the swelling area ratio, we can better interpret the transition between the gas adsorption and the gas absorption. The development of the swelling area is highly related to the average pressure in the coal matrix because the swelling is induced by gas sorption and sorption capacity increases with pressure. The relationship between the matrix swelling area, the pressure in the matrix and permeability reveals the fact that permeability in the fracture is essentially determined by the pressure distribution in the coal matrix rather than that in the fracture.

5.6. Effect of the initial permeability on the evolution of permeability and swelling area ratio

The Critical Swelling Area is not only determined by the pressure in the matrix but also affected by factors like temperature and initial matrix permeability, which is investigated in this and the following sections.

Fig. 10 illustrates the permeability evolution under the constant stress boundary condition. The initial matrix permeability varies from 10^{-22} m^2 to 10^{-20} m^2 when CO_2 is injected at the temperature of 328.15 K into the coal seams with the temperature of 298.15 K. The results show that the initial matrix permeability has significant effects on the evolution of permeability in fracture. The switch of permeability in fracture is observed in all three cases; however, the magnitude of the permeability reduction and the time when permeability switches vary in each case due to the different initial matrix permeability. Permeability in fracture decreases by as much as 35% as the initial permeability is 10^{-22} m^2, 4% more than that in the case with the initial matrix permeability of 10^{-20} m^2. This indicates that the initial matrix permeability affects the amount of the fracture permeability decrease before permeability starts to rebound. The lower the initial matrix permeability, the more the fracture permeability decreases.

Although the fracture permeability in all three cases follows the same trend, namely, a switch from reduction to rebound, the time at which it switches is different. The switch of the fracture permeability in the case with the initial matrix permeability of 10^{-20} m^2 occurs relatively early, at around 3.5×10^3 s, reaching the steady state at around 1.5×10^4 s. The fracture permeability declines with a smaller rate in the case of a lower initial matrix permeability, resulting in a slower evolution of the fracture permeability and a later time for permeability to switch. In the case with the initial permeability of 10^{-22} m^2, the fracture permeability continues to decrease until 7×10^4 s when it starts to recover, reaching the equilibrium after 10^6 s. Noticeably, the permeability switch is sharp in the case with the initial matrix permeability of 10^{-20} m^2, compared to the relatively smooth permeability switch in the other two cases.

These results indicate that the initial matrix permeability not only affects the magnitude of fracture permeability decrease but also has an impact on the time of the permeability evolution. In other words, the lower the initial matrix permeability, the longer it takes for the fracture permeability evolution. Both the variation in the slope of permeability switch and the magnitude of the permeability reduction were attributed to the pressure evolution in the matrix. The more permeability decrease at the switching point in the case with the initial permeability of 10^{-22} m^2 is caused by the higher sorption induced swelling due to the higher pressure in the matrix at the specific time. The permeability switches smoothly from reduction to rebound as the initial matrix permeability is low because of the longer time that the gas diffusion and gas adsorption take.

The initial matrix permeability affects the process of the gas diffusion and gas adsorption in the matrix. If the initial matrix

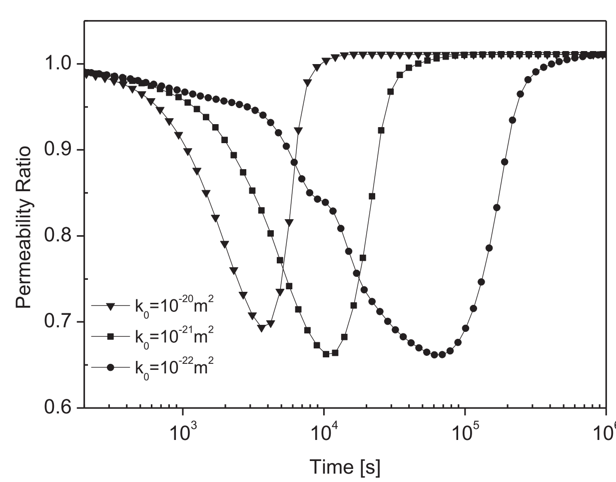

Fig. 10. Evolution of fracture permeability at different initial matrix permeability under the constant stress boundary condition.

permeability is low, the gas flow from fracture to matrix and the gas diffusion within the matrix is slow. Moreover, the coal matrix swelling due to the gas adsorption is impeded by the slow increase of the pressure in the matrix with the gas diffusion. Therefore, the rate of the fracture permeability decrease caused by the local swelling of the coal matrix in the vicinity of the fracture is small and the switch of the permeability is smooth because of the long time it takes for the matrix swelling to change from local to global.

The Critical Swelling Area Ratio at different initial matrix permeability shown in Fig. 11 indicates that the initial matrix permeability affects the Critical Swelling Area Ratio in a significant way. The Critical Swelling Area is high at low initial matrix permeability while it is low at high initial permeability. The Critical Swelling Area Ratio is 13.4% when the initial permeability is 10^{-20} m^2, while it increases to 26.7% and 27.7% respectively as the initial matrix permeability drops to 10^{-21} m^2 and 10^{-22} m^2.

The results demonstrate that under the constant stress boundary condition, the higher the initial matrix permeability, the smaller the Critical Swelling Area. In other words, in the coal with a high initial matrix permeability of 10^{-20} m^2, the swelling of the matrix remains in a relatively small area at the permeability switching point, accounting for 13.4% of the total swelling area when permeability switches from reduction to rebound. However, as the initial matrix permeability decreases to 10^{-21} m^2, permeability does not rebound until the Critical Swelling Area increases to 26.7% of the total swelling area, almost doubling the Critical Swelling Area in the case of 10^{-20} m^2. According to the relationship between permeability, the matrix swelling area and the average pressure in the matrix, the effect of initial matrix permeability on the Critical Swelling Area is attributed to the pressure evolution and gas diffusion in coal matrix, as verified above.

The evolution of the fracture permeability at different initial matrix permeability under the constant volume boundary condition, as illustrated in Fig. 12 demonstrates that the initial matrix permeability has a significant effect on the time of the permeability evolution. Under the constant volume boundary condition, permeability decreases all along by over 90% in three cases and shows no sign of switch as it does in Fig. 10. Although permeability follows similar trend of declining in these three cases, the rate of permeability decrease is different. The fracture permeability with the initial matrix permeability of 10^{-22} m^2 declines slowest among these three cases. With higher initial matrix permeability, the fracture permeability decreases faster. In other words, at any time between the initial and the final state, the fracture permeability with the initial matrix permeability of 10^{-22} m^2, is higher than those in the other two cases.

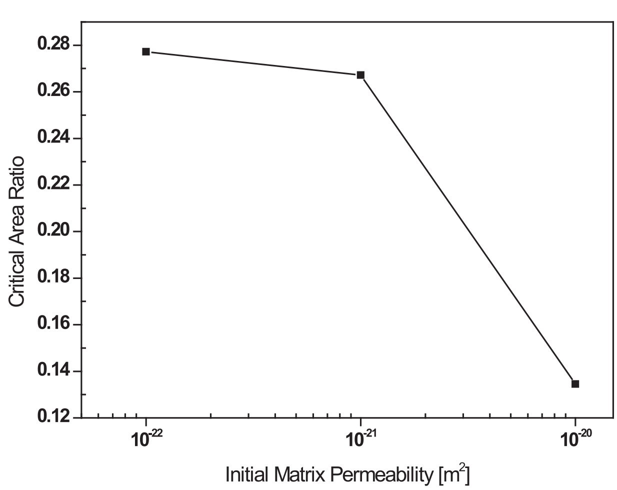

Fig. 11. Critical swelling area ratio at different initial matrix permeability.

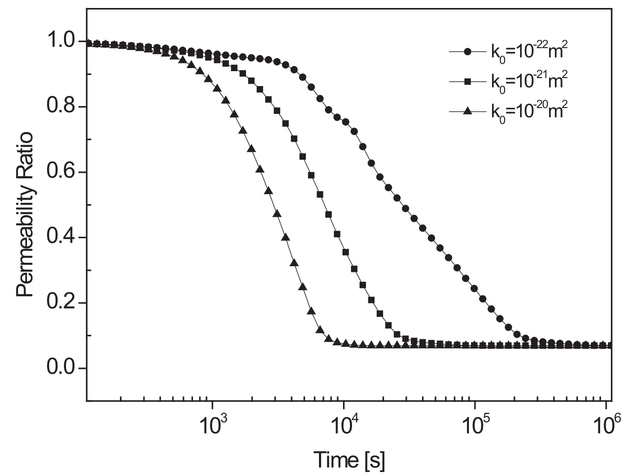

Fig. 12. Evolution of the fracture permeability at different initial matrix permeability under the constant volume boundary condition.

As the initial matrix permeability is 10^{-20} m^2, the fracture permeability ratio decreases rapidly to 0.08 and remains stable at 0.07 after 10^4 s. While in the case with the initial permeability of 10^{-22} m^2, the decrease in the fracture permeability ratio is only 0.20 in the first 10^4 s after which it continues to decrease with the same rate until 2×10^5 s and reaches about 0.07 after 3×10^5 s. It takes about 30 times longer for the fracture permeability to reach the steady state with the initial permeability of 10^{-22} m^2 than with the initial permeability of 10^{-20} m^2 due to the relatively low initial matrix permeability.

The mechanism that causes the fracture permeability to decrease under the constant volume boundary condition is the same mechanism that causes the permeability reduction before the permeability switch under the constant stress condition. The swelling of the coal matrix due to the increase of the gas adsorption in the vicinity of the fracture compresses the fracture and reduces the fracture permeability. Since the permeability with the initial permeability of 10^{-20} m^2 is relatively high, gas diffuses faster from the fracture to the matrix and the pressure in the matrix reaches equilibrium more rapidly. However, there is no permeability rebound due to the constraint of the external boundary.

It is noticeable that the final permeability in these three cases is almost the same even though the initial matrix permeability is different. This result demonstrates that the initial matrix permeability only affects the evolution time of the fracture permeability but has no effect on the magnitude of the permeability change because the initial matrix permeability does not affect the fracture aperture change which determines the fracture permeability. The different initial matrix permeability only results in the different speeds of gas flow and diffusion in the matrix, whereas the amount of gas adsorption and the extent of the matrix swelling are controlled by the pressure in the matrix. Under the same injection pressure and external boundary condition, the fracture permeability at the steady state does not vary with the initial matrix permeability.

5.7. *Effect of temperature on the evolution of permeability and swelling area ratio*

Fig. 13 compares the evolution of the coal permeability ratio under the constant stress boundary condition at three injection temperatures of 278.15 K, 328.15 K and 378.15 K, while the initial temperature in the coal seams remains at 298.15 K.

Permeability decreases faster and rebounds earlier as CO_2 is injected at a low temperature of 278.15 K, compared to those at other two temperatures. Permeability ratio declines gradually and reaches the lowest point of 0.65 at 5×10^4 s and then rebounds and stays stable at 1.01 after 10^6 s. Although the permeability evolution follows the similar trend in the other two cases, the permeability switching time is different in each case. Permeability switches from reduction to rebound at 7×10^4 s and 8×10^4 s respectively as CO_2 is injected at 328.15 K and 378.15 K. Moreover, the magnitude of the maximum permeability decrease is also different in these three cases. In the case of 278.15 K, permeability decreases by 35%, while the permeability reduction is only 32% as CO_2 is injected at 378.15 K. The permeability decrease in the case of 328.15 K is just in between.

The difference in the magnitude of the maximum permeability decrease among different temperature cases is caused by the sorption induced matrix swelling and thermal expansion due to the difference in the injection temperature. On one hand, high temperature induced thermal expansion tends to narrow the fracture aperture during the local swelling process and enhances the permeability decrease. On the other hand, the adsorption capacity decreases with the increase in temperature. The adsorption capacity at 378.15 K is smaller compared to that at 278.15 K, resulting in a less sorption-induced matrix swelling. As a result of the competition of these two combined effects, under the same matrix pressure, the sorption induced matrix swelling at 378.15 K is much smaller than that at 278.15 K. This result, therefore, explains the less permeability decrease at high injection temperature.

Permeability rebounds later at high temperature than it does at low temperature and this is due to the slower increase in the matrix pressure. Temperature causes the coal volume to change through thermal expansion and gas adsorption. Thermal expansion leads to coal swelling at high temperature, whereas the effect of temperature on gas adsorption is more significant. At high temperatures, the adsorption capacity is low and less gas adsorbs on the coal surface thus the pressure in the coal matrix increases slowly, resulting in a slow increase in the fracture permeability.

Fig. 14 shows the effect of temperature on the evolution of the matrix swelling area ratio. The swelling area ratio was compared at three temperatures of 278.15 K, 328.15 K and 378.15 K. With the increase of the temperature, the matrix swelling area ratio decreases, indicating that the higher the temperature, the lower the matrix swelling area ratio. The matrix swelling area ratio remains the highest at 278.15 K, and reaches the steady state the soonest among these three cases, followed by the case at 328.15 K and 378.15 K in sequence. At 10^6 s, the swelling area ratio in the cases of 278.15 K, 328.15 K has almost reached 100% while it is still increasing in the case of 378.15 K. This is caused by the slight difference in the adsorption capacity among these three cases. The adsorption amount in the case of 378.15 K is slightly smaller at 10^6 s compared to those in the cases of 278.15 K and 328.15 K and it takes longer time for the matrix swelling area to reach the equilibrium.

The effect of temperature on the swelling area ratio is attributed to the effect of temperature on adsorption. At high temperature of 378.15 K, the sorption capacity is very low. Only small amount of gas adsorbs on the coal surface, resulting in a small area of coal matrix swelling. As temperature reduces to 278.15 K, the sorption capacity increases, leading to a larger area of coal matrix swelling. Although temperature also affects the coal matrix swelling through thermal expansion, the effect of thermal expansion is rather small compared to the effect of the sorption-induced swelling. The difference in the evolution of the swelling area at different temperatures is primarily caused by the sorption-induced swelling, which outweighs the effect of thermal expansion and dominates the process of permeability evolution.

Fig. 15 illustrates the evolution of the coal permeability ratio under three non-isothermal conditions of 278.15 K, 328.15 K and 378.15 K, under the constant volume boundary condition. The result in this figure is compared with that in Fig. 13. Under the constant volume boundary condition, permeability decreases all along in these three-temperature cases until it reaches equilibrium and remains the highest in the case of the 378.15 K. Permeability follows the same trend of decreasing in these three cases, while the difference among them increases between 10^4 s and 1.5×10^5 s and decreases after that until permeability reaches the equilibrium.

Compared to the permeability evolution under the constant stress boundary condition, there is no permeability switch from reduction to rebound under the constant volume boundary condition. Permeability decreases with an approximate constant rate because the coal sample is fully constrained and no boundary is allowed to move. The sorption-induced matrix swelling caused by the gas adsorption narrows the fracture aperture all the time and reduces the permeability. However, the sorption-induced matrix swelling due to the CO_2 adsorption reduces accordingly with the decrease of adsorption capacity as temperature increases. Therefore, permeability remains higher at the high temperature than that at low temperature.

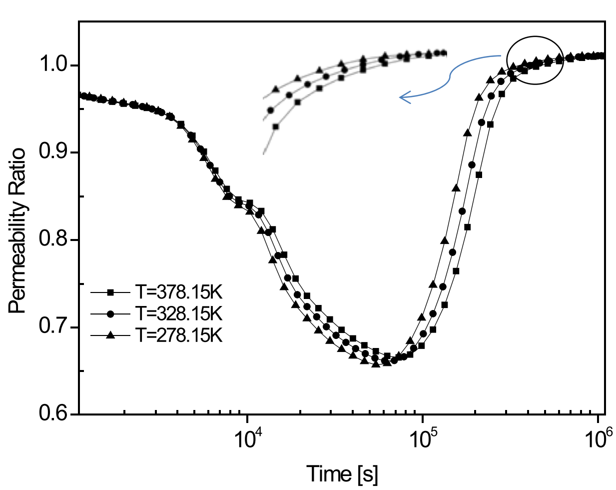

Fig. 13. Evolution of fracture permeability at three temperatures for the CSC.

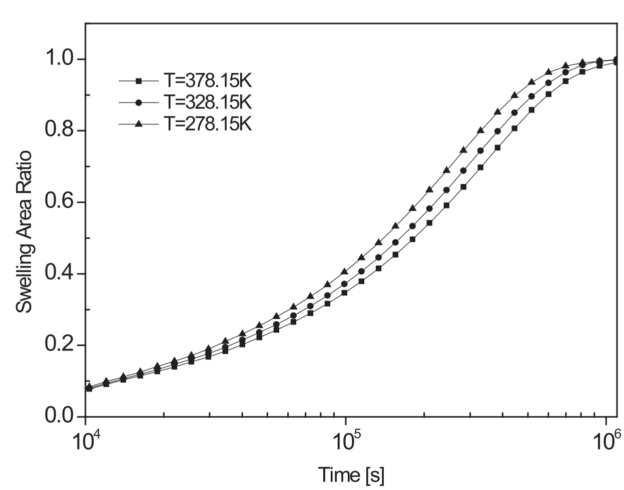

Fig. 14. Evolution of swelling area ratio with time at three temperatures.

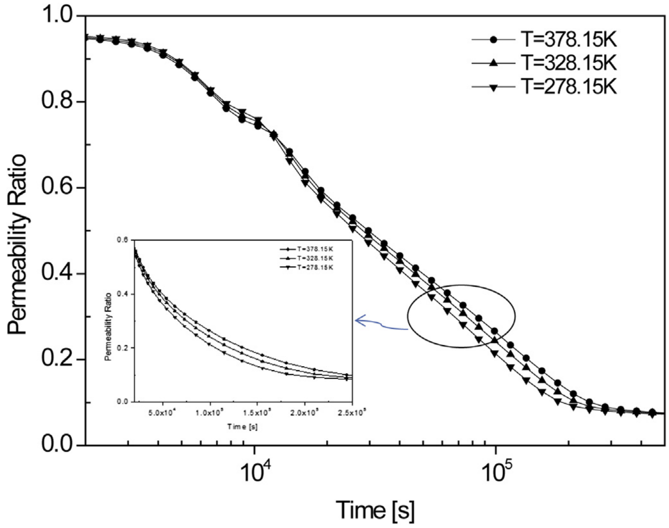

Fig. 15. Evolution of fracture permeability at three temperatures for the CVC.

6. Conclusions

The effect of boundary conditions on permeability was investigated in this study by applying two boundary conditions of constant volume and constant stress to our matrix–fracture interaction model. The Thin Elastic Layer was simulated as the coal bridge in the fracture, and the matrix swelling area was studied to investigate the effect of matrix swelling area on permeability. The concept of Critical Swelling Area is proposed to describe the coal matrix transition from local swelling to global swelling at the permeability switching point. The effect of initial matrix permeability and temperature on the swelling area and permeability evolution was also studied. The main findings are as follows:

6.1. *Effect of boundary condition*

The external boundary condition has great impact on the fracture permeability evolution. Permeability continuously decreases under the constant volume boundary condition while permeability switches from reduction to rebound under the constant stress condition. The fracture is compressed all along under the constant volume condition, leading to the decrease of permeability while the free swelling of the external boundary under the constant stress condition allows the coal bridge to swell together with the matrix at the global swelling, resulting in an increase in the fracture aperture and permeability. The transition of permeability from reduction to rebound under the constant stress condition was explained through the concept of the Critical Swelling Area.

6.2. *Effect of matrix swelling*

Coal matrix swelling is the main reason for permeability evolution. The propagation of the swelling area is highly related to the pressure change in the coal matrix since gas sorption increases with matrix pressure. As the swelling area reaches the Critical Swelling Area, local swelling changes to global swelling. The swelling area is under 50% and the pressure in the matrix remains very low before the permeability switches to rebound, indicating that gas only adsorbs on the coal surface during the local swelling while gas penetrates the coal matrix and absorbs inside the coal matrix at the global swelling stage.

6.3. *Effect of initial matrix permeability and temperature*

The initial matrix permeability and temperature have significant effects on the swelling area ratio and fracture permeability evolution. The initial matrix permeability affects both permeability evolution time and the magnitude of permeability change. With lower initial matrix permeability, it takes longer time for the permeability evolution and the Critical Swelling Area Ratio at the permeability switching point is relatively high. Temperature affects permeability through sorption induced swelling and thermal expansion. At high temperature, permeability decreases less due to the decrease in sorption induced swelling since the reduction in adsorption strain outweighs the increase in thermal strain caused by thermal expansion.

Acknowledgments

This work is partially funded by the Chinese Scholarship Council and the Australia–China Natural Gas Technology Partnership Fund through scholarships, the Foundation of State Key Laboratory of Petroleum Resources and Prospecting, China University of Petroleum, Beijing, (PRP/indep-4-1314), State Key Laboratory of Coal Resources and Safe Mining of China University of Mining and Technology (SKLCRSM11KFA01), and the State Administration of Foreign Experts Affairs, PR China (TS2011ZGKY[BJ]019). These supports are gratefully acknowledged.

References

Clarkson, C.R., Jordan, C.L., Gierhart, R.R., Seidle, J.P., 2008. Production data analysis of coalbed-methane wells. SPE Reserv. Eval. Eng. 11 (2), 311–325.
Clarkson, C.R., Pan, Z., Palmer, I.D., Harpalani, S., 2010. Predicting sorption-induced strain and permeability increase with depletion for coalbed-methane reservoirs. SPE J. 15 (1), 152–159.
Connell, L.D., Detournay, C., 2009. Coupled flow and geomechanical processes during enhanced coal seam methane recovery through CO_2 sequestration. Int. J. Coal Geol. 77, 222–233.
Connell, L.D., Lu, M., Pan, Z., 2010. An analytical coal permeability model for tri-axial strain and stress conditions. Int. J. Coal Geol. 84 (2), 103–114.
Cui, X., Bustin, R.M., 2005. Volumetric strain associated with methane desorption and its impact on coalbed gas production from deep coal seams. AAPG Bull. 89, 1181–1202.
Gray, I., 1987. Reservoir engineering in coal seams: part 1-the physical process of gas storage and movement in coal seams. SPE Reserv. Eng. 2, 28–34.
Harpalani, S., Chen, G., 1995. Estimation of changes in fracture porosity of coal with gas emission. Fuel 74 (10), 1491–1498.
Harpalani, S., Chen, G., 1997. Influence of gas production induced volumetric strain on permeability of coal. Geotech. Geol. Eng. 15, 303–325.
Izadi, G., Wang, S., Elsworth, D., Liu, J., Wu, Y., Pone, D., 2011. Permeability evolution of fluid-infiltrated coal containing discrete fractures. Int. J. Coal Geol. 85 (2), 202–211.
Kiyama, T., Nishimoto, s, Fujioka, M., Xue, Z., Ishijima, Y., Pan, Z., Connell, L.D., 2011. Coal swelling strain and permeability change with injecting liquid/supercritical CO_2 and N_2 at stress-constrained conditions. Int. J. Coal Geol. 85, 56–64.
Liu, H.H., Rutqvist, J., 2010. A new coal-permeability model: internal swelling stress and fracture–matrix interaction. Transp. Porous Media 82, 157–171.
Liu, J., Chen, Z., Elsworth, D., Miao, X., Mao, X., 2010a. Evaluation of stress-controlled coal swelling processes. Int. J. Coal Geol. 83, 446–455.
Liu, J., Chen, Z., Elsworth, D., Qu, H., Chen, D., 2011a. Interactions of multiple processes during CBM extraction: a critical review. Int. J. Coal Geol. http://dx.doi.org/10.1016/j.coal. 2011.06.004.
Liu, J., Wang, J., Chen, Z., Wang, S., Elsworth, D., Jiang, Y., 2011b. Impact of transition from local swelling to macro swelling on the evolution of coal permeability. Int. J. Coal Geol. 88, 31–40.
Liu, J., Chen, Z., Elsworth, D., Miao, X., Mao, X., 2011c. Evolution of coal permeability from stress-controlled to displacement-controlled swelling conditions. Fuel 90, 2987–2997.
Liu, S.M., Harpalani, S., 2013a. A new theoretical approach to model sorption-induced coal shrinkage or swelling. Aapg Bulletin 97, 1033–1049.
Liu, S.M., Harpalani, S., 2013b. Permeability prediction of coalbed methane reservoirs during primary depletion. International Journal of Coal Geology 113, 1–10.
Liu, S., Harpalani, S., Pillalamarry, M., 2012. Laboratory measurement and modeling of coal permeability with continued methane production: Part 2 – modeling results. Fuel 94, 117–124.

Ma, Q., Harpalani, S., Liu, S., 2011. A simplified permeability model for coalbed methane reservoirs based on matchstick strain and constant volume theory. Int. J. Coal Geol. 85, 43–48.
Massarotto, P., Golding, S.D., Rudolph, V., 2009. Constant volume CBM reservoirs: an important principle. In: 2009. International Coalbed Methane Symposium, Tuscaloosa, Alabama. Paper 0926.
Mazumder, S., Wolf, K.H., 2008. Differential swelling and permeability change of coal in response to CO_2 injection for ECBM. Int. J. Coal Geol. 74, 123–138.
Mitra, A., Harpalani, S., Liu, S., 2012. Laboratory measurement and modeling of coal permeability with continued methane production: part 1 – laboratory results. Fuel 94, 110–116.
Moffat, D.H., Weale, K.E., 1955. Sorption by coal of methane at high pressures. Fuel 34, 449–462.
Palmer, I., Mansoori, J., 1996. How Permeability Depends on Stress and Pore Pressure in Coalbeds: a New Model, SPE Annual Technical Conference and Exhibition, 1996 Copyright 1996. Society of Petroleum Engineers, Inc., Denver, Colorado.
Palmer, I., Reeves, S.R., 2007. Modeling Changes of Permeability in Coal Seams. Final Report, DOE Contract No. DE-FC26–C00NT40924, July, 2007.
Palmer, I., Mavor, M., Gunter, B., 2007. Permeability Changes in Coal Seams during Production and Injection. Paper 0713 Presented at the International Coalbed Methane Symposium, Tuscaloosa, Alabama, USA, 5–9 May.
Pan, Z., Connell, L.D., 2007. A theoretical model for gas adsorption-induced coal swelling. Int. J. Coal Geol. 69 (4), 243–252.
Pan, Z., Connell, L.D., 2011. Modelling of anisotropic coal swelling and its impact on permeability behaviour for primary and enhanced coalbed methane recovery. Int. J. Coal Geol. 85, 257–267.
Pan, Z., Connell, L.D., 2012. Modelling permeability for coal reservoirs: a review of analytical models and testing data. Int. J. Coal Geol. 92, 1–44.
Pan, Z., Connell, L.D., Camilleri, M., 2010. Laboratory characterisation of coal reservoir permeability for primary and enhanced coalbed methane recovery. Int. J. Coal Geol. 82, 252–261.
Pekot, L.J., Reeves, S.R., 2002. Modeling the Effects of Matrix Shrinkage and Differential Swelling on Coalbed Methane Recovery and Carbon Sequestration. U.S. Department of Energy. DE-FC26–00NT40924.
Pini, R., Ottiger, S., Burlini, L., Storti, G., Mazzotti, M., 2009. Role of adsorption and swelling on the dynamics of gas injection in coal. J. Geophys. Res. 114, B04203.
Qu, H., Liu, J., Chen, Z., Wang, J., Pan, Z., Connell, L., Elsworth, D., 2012. Complex evolution of coal permeability during CO_2 injection under variable temperatures. Int. J. Greenh. Gas. Control 9, 281–293.
Robertson, E.P., 2005. Modeling permeability in coal using sorption-induced strain data. In: SPE Annual Technical Conference and Exhibition. Society of Petroleum Engineers, Dallas, Texas.
Robertson, E.P., Christiansen, R.L., 2006. A permeability model for coal and other fractured, sorptive-elastic Media. In: SPE Eastern Regional Meeting. Society of Petroleum Engineers, Canton, Ohio, USA.
Seidle, J.R., Huitt, L.G., 1995. Experimental measurement of coal matrix shrinkage due to gas desorption and implications for fracture permeability increases. In: International Meeting on Petroleum Engineering. Society of Petroleum Engineers, Inc., Beijing, China, 1995 Copyright 1995.
Shi, J.Q., Durucan, S., 2004a. A numerical simulation study of the Allison unit CO_2 -ECBM pilot: the impact of matrix shrinkage and swelling on ECBM production and CO_2 injectivity. In: Proceedings of 7th International Conference on Greenhouse Gas Control Technologies.
Shi, J.Q., Durucan, S., 2004b. Drawdown induced changes in permeability of coalbeds: a new interpretation of the reservoir response to primary recovery. Transp. Porous Media 56, 1–16.
Siriwardane, H., Haljasmaa, I., McLendon, R., Irdi, G., Soong, Y., Bromhal, G., 2009. Influence of carbon dioxide on coal permeability determined by pressure transient methods. Int. J. Coal Geol. 77, 109–118.
Viete, D.R., Ranjith, P.G., 2006. The effect of CO2 on the geomechanical and permeability behaviour of brown coal: implications for coal seam CO2 sequestration. Int. J. Coal Geol. 66, 204–216.
Vishal, V., Ranjith, P.G., Pradhan, S.P., Singh, T.N., 2013a. Permeability of sub-critical carbon dioxide in naturally fractured Indian bituminous coal at a range of down-hole stress conditions. Eng. Geol. 167, 148–156.
Vishal, V., Ranjith, P.G., Singh, T.N., 2013b. CO_2 permeability of Indian bituminous coals: implications for carbon sequestration. Int. J. Coal Geol. 105, 36–47.
Wang, G.X., Wei, X.R., Wang, K., Massarotto, P., Rudolph, V., 2010. Sorption-induced swelling/shrinkage and permeability of coal under stressed adsorption/desorption conditions. Int. J. Coal Geol. 83 (1), 46–54.